Sonneck-Museux N., Scheer E., Perez L., Autrique L., Agay D., *Development of a Skin Burn Predictive Model adapted to Laser irradiation*, International Journal of Thermophysics, 37 n°12, pp 1-23, 2016.

Development of a Skin Burn Predictive Model adapted to Laser Irradiation

N. Sonneck-Museux[1], E. Scheer[1], L. Perez[2], D. Agay[3] and L. Autrique[4]

[1] DGA/TA/MT/MTO, 10 rue des fours solaires, BP 59, 66121 Font-Romeu, France

[2] LTN, UMR-CNRS 6607, rue Christian Pauc, BP 50609, 44306 Nantes cedex 3, France

[3] CEA-Leti-Clinatec, 17 rue des Martyrs, 38054 Grenoble Cedex 9, France

[4] LARIS, University of Angers, 62 avenue Notre Dame du Lac, 49000 Angers, France

Abstract Laser technology is increasingly used and it is crucial for both safety and medical reasons that the impact of laser irradiation on human skin can be accurately predicted. This study is mainly focused on laser-skin interactions and potential lesions (burns). A mathematical model dedicated to heat transfers in skin exposed to infrared laser radiations has been developed. The model is validated by studying heat transfers in human skin and simultaneously performing experimentations an animal model (pig). All along the experimental tests, pig's skin surface temperature is recorded. Three laser wavelengths have been tested: 808, 1940 and 10 600 nm. The first is a diode laser producing radiation absorbed deep within the skin. The second wavelength has a more superficial effect. For the third wavelength, skin is an opaque material. The validity of the developed models is verified by comparison with experimental results (*in-vivo* tests), and the results of previous studies reported in the literature. The comparison shows that the models accurately predict the burn degree caused by laser radiation over a wide range of conditions. The results show that the important parameter for burn prediction is the extinction coefficient. For the 1940 nm wavelength especially, significant differences between modeling results and literature have been observed, mainly due to this coefficient's value. This new model can be used as a predictive tool in order to estimate the amount of injury induced by several types (couple power-time) of laser aggressions on the arm, the face and on the palm of the hand.

Keywords: experimentation *in vivo*; laser irradiation; skin burn; thermal modeling

1 Introduction

In the military context, laser based devices are widespread for guidance systems, measurement devices, weapons, etc. Laser technologies are also used in other domains, such as medicine, dermatology, surgery and several industrial fields, where accidental exposure or misuse can induce damage in the skin or the eyes [1]. Numerous authors have studied these points, but the effects of laser on skin seem less well investigated. Thermal damage to the skin occurs with the local absorption of laser radiations, which are converted into heat. The generated damage strongly depends on the wavelengths. In this context, this study is the continuation of the previous paper concerning analysis and predictive simulation of laser irradiations thermal effects on skin [2]. In the previous study, two lasers (wavelength 808 nm and 1940 nm) were investigated and histological analysis was performed. In the following, results are presented considering an additional CO_2 laser. This laser is specific since for such 10 600 nm wavelength, skin is an opaque material. Thus new experimental results are analyzed. Moreover in the predictive mathematical model which is implemented for numerical simulation, water losses is described in order to take into account the modification of biological tissues thermal characteristics. Last but not least, from the experimental view, optical device developed for pig skin laser irradiation is modified. In [2] a large kaleidoscope (square section: 20cmx20cm) was used and metallic edges were in contact with studied pig skin. Such configurations slightly modify the heat transfers near the burn area boundaries. In the following a small kaleidoscope is used (square section: 4mmx4mm) and combined with a proper lens in order to avoid skin contact while obtaining a large burn area.

Over two hundred experiments on pig skin considering three lasers of 808, 1940 and 10 600 nm wavelengths are performed. The radiation of the first laser is absorbed by melanin. Since its absorption coefficient is low then 808 nm laser effects is not limited to skin's superficial layers. Medical and cosmetic applications of such lasers are various: reduction of pigmentation, tattoo removal, treatment of retina disease, removal of unwanted hair, etc. The second laser (1940 nm) acts on the skin surface. It is used in emerging applications for 2 µm fiber lasers in medicine and surgery [3]. For such a wavelength, laser radiation does not penetrate deeply into the skin [4, 5]. Medical applications are ophthalmology (presbyopia, hyperopia), otolaryngology, orthopedic procedures, etc. The third laser tested in this study is a CO_2 laser which beam is generated by gas excitation. It is used for tattoo removal, scars treatment, artery and vein malformations treatment and for resurfacing [6-8] and can be used for rejuvenation purposes. For both 1940 nm and 10.6 µm's radiation, chromophore is water. Due to their different absorption coefficients, effects of 1940 nm laser are deeper in skin than effects of 10.6 µm laser [9].

The aim of presented experimentations is to study burns caused by laser. The selected animal model is the pig since this mammal is usually considered as an adequate test animal when a high level of similarity with human skin is required [10]. Based on experimentations results, damages caused by these three infrared wavelengths are compared.

Since pioneer works [11] developed by Pennes in 1948, numerous authors have investigated heat transfer in living tissues. In a first mathematical model based on tests by Chen et al. [5, 12], effect of potential water losses has not been considered. In the present study, considerations related to these losses have been added in order to enrich the predictive mathematical model devoted to

thermal effects prediction induced by a laser occurrence. Several additional phenomena are taken into account: convection, radiation, evaporation on skin surface and heat losses due to blood circulation [2].
The paper is organized as follows. Firstly, the propagation of the laser beam in the skin layers is described. A brief paragraph related to water losses effect is presented. Then, *in vivo* experimentations are briefly described; pig skin temperature is measured in order to evaluate injuries in comparison with temperature evolution. Adequacy between observed effect and predicted effect based on mathematical model is discussed and several simulation results on other body parts are presented as an application of this model.

2 Mathematical model - Heat Transfers

2.1 Background

The skin is a multilayer semi-transparent material and it is usual to consider three layers: epidermis, dermis and hypodermis. The model presented hereafter is based on the Pennes heat transfer equation in biological tissues [11]. Considering heat conduction, laser radiation, blood circulation and heat generation due to metabolism, the following equation is taken into account:

$$\rho_i c_i \frac{\partial T(x,t)}{\partial t} = k_i \Delta T(x,t) + \omega_i \rho_b c_b \left[T_b - T(x,t)\right] + q_m + S\left(x,t\right) \quad (1)$$

where *T(x,t)* is the temperature in (K) at depth x in (m) and time t in (s), $i \in \{e,d,h\}$ corresponds to a specific layer: epidermis $\{e\}$, dermis $\{d\}$ or hypodermis $\{h\}$, ρ_i is the density in (kg.m^{-3}) of layer i, ρ_b is blood density in (kg.m^{-3}), c_i is the specific heat in (J.kg^{-1}.K^{-1}), k_i is the thermal conductivity in (W.m^{-1}.K^{-1}), T_b is the blood temperature (K) assumed to be constant, q_m is the heat generation due to the metabolism, ω_i is the blood perfusion rate in dermis and hypodermis (in s^{-1}) and is equal to zero in the epidermis. Laser radiation effect is described by:

$$S\left(x,t\right) = \beta_{i,\lambda} I\left(t\right) \exp\left(-\beta_{i,\lambda} x\right) \quad (2)$$

where $\beta_{i,\lambda}$ in (m^{-1}) is the wavelength-dependent absoprtion coefficient of layer i for a given laser wavelength (1940 nm or 10600 nm), $I\left(t\right)$ is the laser irradiance (W.m^{-2}).
Parametric evaluation of tissue damage was investigated in 1947 by Henriques and Moritz in a series of key papers [13, 14]. In their works, thermal damage was estimated using a dimensionless positive function $\Omega\left(x,t\right)$, given by the following Arrhenius equation:

$$\Omega\left(x,t\right) = A\int_0^t \exp\left(\frac{-E_a}{R\,T\left(x,\tau\right)}\right) d\tau \quad (3)$$

where A is a pre exponential factor (s^{-1}), E_a is the activation energy (J.mole^{-1}) and R is the universal gas constant (8.32 J.mole^{-1}.K^{-1}). One can notice that the pre exponential factor A can be defined as a molecular collision frequency.
While studying *in vivo* pig skin temperature, during a burn induced by hot water, Henriques and Moritz defined three values of Ω corresponding to three burn degrees [19]:

- $0.53 \le \Omega(x,t) < 1$ describes a first degree burn,
- $1 \le \Omega(x,t) < 10000$ is the range for second degree burn,
- $10000 \le \Omega(x,t)$ corresponds to a third degree burn.

A discussion concerning A and E_a parameters is proposed in [2].
In order to improve understanding related to heat transfer in skin during laser occurrence, several points have to be specifically discussed.

2.2 Blood perfusion

In Eq. (1), the term $\omega_i \rho_b c_b \left[T_b - T(x,t)\right]$ describes the heat increase in the dermis and hypodermis if the blood temperature is greater than $T(x,t)$. If the blood temperature is lower than $T(x,t)$ then blood circulation induces a cooling effect. This term used in Pennes bioheat equation to describe blood perfusion has been considered in numerous studies. However it is obvious that pioneer investigations performed by Pennes about analysis of tissue and arterial blood temperature in the resting human forearm is not adapted to specific configurations. For example, Pennes's model does not take into account a number of factors, including directional dependence of perfusion heat source, different diameters of blood vessels, sharply varying material properties, heat generation by necrosis, vasculature geometry, and transvascular transport of energy and mass.
Thus, various improvements have been proposed in the literature. For example, in [15] effect of increasing blood perfusion rate is highlighted and it is shown how blood can acts as a heat source rather than a heat sink. In [16] microvascular contributions in tissue heat transfer are investigated. Such study is more adapted to blood perfusion in dermis and hypodermis considering additional terms: the first one is proportional to local blood perfusion velocity while the second one takes into account the effective thermal conductivity. This last term is quite difficult to evaluate considering anisotropic arrangement of microvasculature. In [17] a vascular based model is presented where the variation of the vascular geometry as a function of tissue depth is detailed. Description of blood perfusion in mathematical predictive model is still a current topic of interest and in [18-21] this parameter depends on temperature in order to describe specifics case of temperature-dependent perfusion. In [22] the human blood circulatory system is described considering countercurrent heat exchanges in order to obtain a more realistic distribution of the arterial blood temperature T_b. In such a model, the countercurrent heat exchange coefficient is difficult to estimate and strongly depends on the body part.
In spite of numerous improvements to the models, the adequacy of the models for predicting the effects of burns produced by lasers is still open to question. Stress as well as development of charateristic lesions could significantly modified blood perfusion. Thus Pennes Bio heat equation is considered as a standard model but adapted to burn process.
Blood circulation is modified during burn process and in [23] Abraham and Sparrow have proposed a relation between blood circulation (ω_i) and tissues damage (Ω). In the following, blood perfusion throughout the heating process for a porcine model [24] has been modeled as

follows.

$$\omega(\Omega) = (1 + 25\Omega - 260\Omega^2)\omega_0 \quad \Omega \in [0, 0.1] \tag{4}$$

$$\omega(\Omega) = (1 - \Omega)\omega_0 \quad \Omega \in]0.1, 1] \tag{5}$$

$$\omega(\Omega) = 0 \quad \Omega > 1 \tag{6}$$

In Eq. 4, an increase in the perfusion rate is recorded as tissue is moderately heated, with vasodilation due to inflammation. In the Eq. 5 while the heating process persists, blood flow decreases as the vasculature begins to shut down (thrombosis/necrosis) (Eq. 6). The term ω_0 is the rate of perfusion in totally undamaged tissue [14, 25]. According to the referenced works, ω_0 is 8.3 10^{-3} s^{-1} in the dermis (5.3 10^{-3} s^{-1} in the hypodermis).

2.3 Heat exchanges on skin surface

Heat exchanges on skin surface $(x = 0)$ have to take into account:

- convective heat transfers which are described by $\mathrm{h}(T_a - T(0,t))$ where h is the heat transfer coefficient, T_a is the external temperatures (room temperature) and $T(0,t)$ is the skin surface temperature.
- radiative heat losses which are described by $\sigma\varepsilon\left(T_a^4 - \left(T(0,t)\right)^4\right)$ where $\varepsilon = 0.97$ is the emissivity and $\sigma = 5.67\ 10^{-8}$ $W.m^{-2}.K^{-4}$ is the Stefan-Boltzmann constant.

Such grey-box models are widely used in thermal sciences [26, 27]. Then heat exchanges on skin surface can be described as follows:

$$\begin{aligned}\mathrm{h}(T_a - T(0,t)) + \sigma\varepsilon\left(T_a^4 - \left(T(0,t)\right)^4\right) &= \mathrm{h}(T_a - T(0,t)) + \sigma\varepsilon(T_a - T(0,t))(T_a + T(0,t))\left(T_a^2 + \left(T(0,t)\right)^2\right) \\ &= \left(\mathrm{h} + \sigma\varepsilon(T_a + T(0,t))\left(T_a^2 + \left(T(0,t)\right)^2\right)\right)(T_a - T(0,t)) \\ &= h_e(T)(T_a - T(0,t))\end{aligned}$$

For free convection in air, heat transfer coefficient h usually ranges between 5 to 25 $W.m^{-2}.K^{-1}$. Thus, as $T_a \approx 290\,\mathrm{K}$ and $T(0,t) \in [290, 390]$, then $h_e(T)$ ranges from 10 to 35 $W.m^{-2}.K^{-1}$. Considering the specific experimental conditions let us assume that $h_e(T)$ is small and the following value is proposed:

$$h_e(T) = \mathrm{h_e} = 10\ W.m^{-2}.K^{-1}.$$

Evaporative cooling and heat losses due to water vaporization are defined as follows:

$$Q_{vap}(t) = \mathrm{H}\ \mathrm{h_m}\left(\rho_{v,sat}(T(0,t)) - \rho_{v,a}\right) \tag{7}$$

where Q_{vap} is in ($W.m^{-2}$), H is the phase change enthalpy ($J.kg^{-1}$), $\mathrm{h_m}$ is the convection mass transfer coefficient ($m.s^{-1}$), $\rho_{v,a}$ is the density of the water vapor in the air ($kg.m^{-3}$) at ambient temperature T_a and $\rho_{v,sat}$ is the mass density of saturated water vapor ($kg.m^{-3}$) at skin surface

temperature $T_s = T(0,t)$. In [20, 28] for example, such phenomenon is taken into account in order to describe the thermal response of tissue affected by laser irradiation.
Considering the previous remarks, heat exchanges on skin surface $(x = 0)$ are globally described by the following boundary condition.

$$-k_e \left.\frac{\partial T}{\partial x}\right|_{x=0} = h_e \left(T_a - T(0,t)\right) - Q_{vap}(t) \tag{8}$$

Inside the porcine body (deeper than the hypodermis layer), a constant temperature (Dirichlet condition) is considered and assumed to be equal to the blood temperature T_b.

2.4 Water losses – description and effect

Water is crucial to ensure skin viability. It follows a specific path through the different cutaneous layers: it circulates through blood vessels until it reaches dermis, where glycosaminoglycans are able to attract water. Then, water is distributed from dermis to epidermis in order to maintain cutaneous hydration. According to Takata [30], the density (ρ_i in kg.m^{-3}), the specific heat (C_i in J.kg^{-1}.K^{-1}) and the thermal conductivity (k_i in W.m^{-1}.K^{-1}) of skin layer *i* depend of hydration rate (w_i) considering following equations:

$$C_i = \left(1.55 + 2800\frac{w_i}{\rho_i}\right)10^3 \tag{9}$$

$$\rho_i = (1.3 - 0.3w_i)10^3 \tag{10}$$

$$k_i = \left(0.06 + 570\frac{w_i}{\rho_i}\right) \tag{11}$$

For Zhang et al. [31], the specific heat and the thermal conductivity depends on both the hydration rate and the layer temperature:

$$C_i = 4190\left(0.37 + 0.63w_i\left(1 + 1.016(T - 293)10^{-4}\right)\right) \tag{12}$$

$$k_i = 0.419\left(0.133 + 1.36w_i\left(1 + 1.78(T - 293)10^{-3}\right)\right) \tag{13}$$

In [31], the mass of the water in the tissues is taken to be 69 % of the total tissue mass. However spatial distribution of water (versus skin depth) is not constant and depends on the skin layer. For example, it is relevant to consider that in epidermis due to heat transfer with ambient environment w_i could be reduced. In hypodermis, adipocytes (cells that primarily compose adipose tissue) have hydrophobic characteristics and then hydration rate in hypodermis is lower than inside the dermis. Considering the previous comments, references [32, 33], the skin thermal properties $(\rho_i C_i$ and $k_i)$ given in [2] and that it is crucial to determine with a good accuracy $\rho_h C_h$ and $\rho_d C_d$ (see [34]) the following values are considered :

- in epidermis : w_i = 30%
- in dermis : w_i = 80%
- in hypodermis : w_i = 20%

Equations (12-13) do not induce a meaningful variation for $\rho_i C_i$ while thermal conductivity is

more affected by thermal variation (in the temperature range $T \in [293,373]$). However, this thermal conductivity variation is lower than 13% and it has been shown in [34] that such uncertainties do not dramatically affect temperature prediction. Thus, in this model, it is Eq. 9 -11 which are used, because $\rho_i C_i$ do not depend on the skin temperature.

In order to observe the water influence on skin temperature, experimentations on dead pig rind were performed. Three samples were used: the first weighed 31.44 g and was stored in a refrigerator, the second weighed 30.20 g and was submerged in water at room temperature, and finally, the third weighed 29.81 g and was kept in free air. After 36 hours, respective weights were 28.49 g, 38.26 g and 23.92 g, so the weight of moisturized pig rind has increased by 26.7% while the weight of dehydrated (in free air) and intermediate (in refrigerator) rind has decreased by 19.7 and 9.4%. Table 1 summarizes tested conditions. Fig. 1 and 2 shows temperature results in surface during 20s laser experimentation (two wavelengths are tested).

Table 1 Experimentations on pig rind for water rate effect

Laser (nm)	**Duration (s)**	**Irradiance (x 10^4 W.m^{-2})**	**Pig rind state**
10600	10	1.5	Dehydrated
	10	1.5	Moisturized
	20	1.0	Dehydrated
	20	1.0	Moisturized
1940	10	1.3	Dehydrated
	10	1.3	Moisturized
	20	0.9	Dehydrated
	20	0.9	Moisturized
	20	0.9	Intermediate

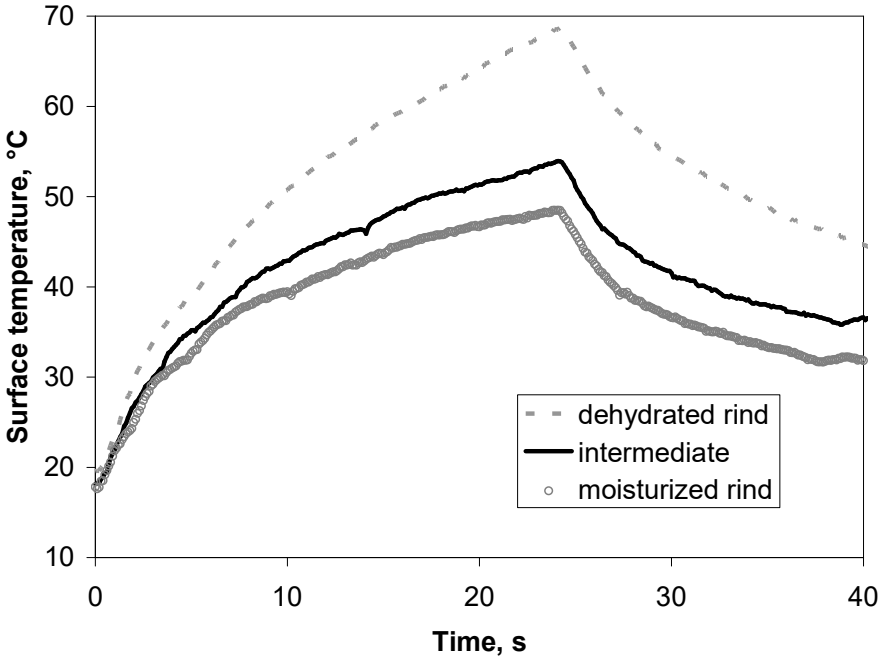

Fig 1. Pig rind surface temperature versus time for a test of 0.9 10^4 W.m^{-2} during 20 s with a 1940 nm laser.

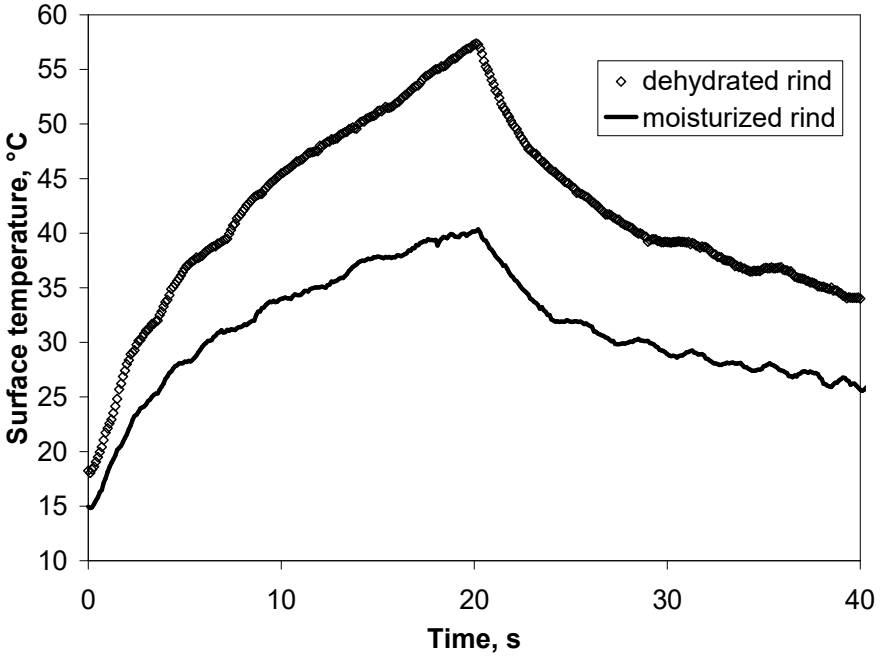

Fig. 2. Pig rind surface temperature versus time for a test of 1.0 10^4 W.m^{-2} during 20 s with a 10.6 µm laser.

On Fig. 1 it is shown that for an irradiation with the 1940 nm laser during 20 s, skin surface temperature increase rises to 342K for the moisturized rind while for the dehydrated rind the temperature rises to 320K. On Fig. 2, with the 10600 nm laser skin surface temperature increase rises to 330K for the moisturized rind while for the dehydrated rind the temperature rises to 313K. Results confirm influence of water in tissue: the lesser the moisture rate, the higher the surface temperature. So, the importance of skin lesion will depend on skin moisture.

In addition with the modification of the thermal properties of skin layers, hydration rate which describes the water content, also affects the optical properties. The primary absorber (chromophore) at 1940 nm and 10.6 µm wavelength is water. Considering that light scattering is not significant for such wavelengths, light propagation in the skin mainly depends on wavelength-dependent absorption coefficient. In [33] Chen et al. estimate that the absorption coefficient is based on the product of water absorption coefficient (μ_{water} in m^{-1}) and the water content in the *i* layer (w_i):

$$\beta_{i,\lambda} = \mu_{water,\lambda} \times w_i \tag{14}$$

In order to simulate water content evolution during a laser shot, a thermogravimetry study was carried out considering pig rind. In each layer (epidermis, dermis, hypodermis) w_i depends on temperature (T) and on time (t in s). Evolution of water content from initial hydration rate (given in Table 2) is:

$$w_i = w_{i,\text{initial}} \qquad 273\ \text{K}<T<293\ \text{K} \tag{15}$$

$$w_i(T) = w_{i,\text{initial}} \times \left(1-\left(0.0068T-2\right)\right) \qquad 293\ \text{K}<T\leq 343\ \text{K} \tag{16}$$

$$w_i(t) = w_i(343K) \times \left(1-0.162\left(t-t_{343}\right)\right) \qquad T>343\ \text{K} \tag{17}$$

where t_{343} is the time for which skin temperature is equal to 343K. The previous equations are related to short irradiation duration (lower than 20s) and describe irreversible water loss during the heating phase.

Considering the previous Eq. related to Pennes bioheat equation, burn degrees estimation, blood perfusion depending on injury severity, and the effect of hydration rate on both thermal characteristics and skin layer absorption coefficient, a numerical predictive model can be implemented in order to estimate temperature evolution inside the skin and the burn degree versus depth and time. Thermal and optical properties used in the mathematical model are presented in Table 2. Skin layers thickness corresponds to arm skin.

Table 2 Thermal and optical properties used in the mathematical model

Properties		Location	Value	Reference
Thickness ($\times 10^3$ m)		Epidermis Dermis Hypodermis	0.1 1.4 > 3.0	Experimental measurement
Specific heat C (J.kg^{-1}.K^{-1})		Epidermis Dermis Hypodermis	Eq. 9	[30]
		Blood	3300	[13]
Thermal conductivity k (W.m^{-1}.K^{-1})		Epidermis Dermis Hypodermis	Eq. 10	[30]
Density ρ (kg.m^{-3})		Epidermis Dermis Hypodermis	Eq. 11	[30]
		Blood	1080	[13]
Initial hydration rate $w_{i,initial}$ (%)		Epidermis Dermis	30 80	[33]
		Hypodermis	20	[32]
Absorption and scattering coefficient β (m^{-1}) at 808 nm		Epidermis Dermis Hypodermis	1000 800 800	[25,36]
Absorption coefficient of water μ_{water} (m^{-1})	1940 nm		6912	[33]
	10.6 µm		85480	
Heat transfer coefficient h_e (W.m^{-2}.K^{-1})			10	
Ambient temperature T_a (K)			295.5	Experimental measurement

3 Animal Experimentations

The damage caused by laser exposure was investigated *in vivo*. Pigs were exposed to laser radiation at three wavelengths; 808 nm, 1940 nm and 10.6 µm, and the skin-temperature evolutions were measured. Tissue biopsies were also performed to assess the depth of the burn injuries.

3.1 Test bench

Three lasers were considered for experimentations. The first one was an infrared fiber laser (1940 nm - IPG photonics, Model TLR-3, maximum power 4 W) while the second one was a

diode near infrared laser (808 nm - Optotools, type OTF 60-30 system, maximum power 60 W). Finally, the third is a CO_2 laser (Millenium lasers LTD, Model ML30/S, maximum power 40 W). In Chen et al. [5], Gaussian shaped spot sizes are approximately 5, 10 and 15 mm. An optical device has been developed which transforms the Gaussian type laser beam into a uniform spatial distribution [35]. It consists in a kaleidoscope (polished aluminum) located after the laser. Its dimensions are 80 mm length with a square cavity of 4 by 4 mm. An additional lens is used in order to obtain a large irradiated zone (with a uniform spatial distribution). The three lasers were triggered by a function generator (FG 120 Yokogawa, 2MHz). The surface temperature of pig skin was measured by an infrared pyrometer (Ultrakust Thermophil INFRAplus®, type R2510-10, focal distance 360 mm in range 8-14 µm, temperature scale 0-200°C). Temperature evolutions were monitored all along the experimentations (oscilloscope Tektronix DPO 4104 or Nicolet Technologies, VISION XP). Experimental setup is briefly described Fig. 3.

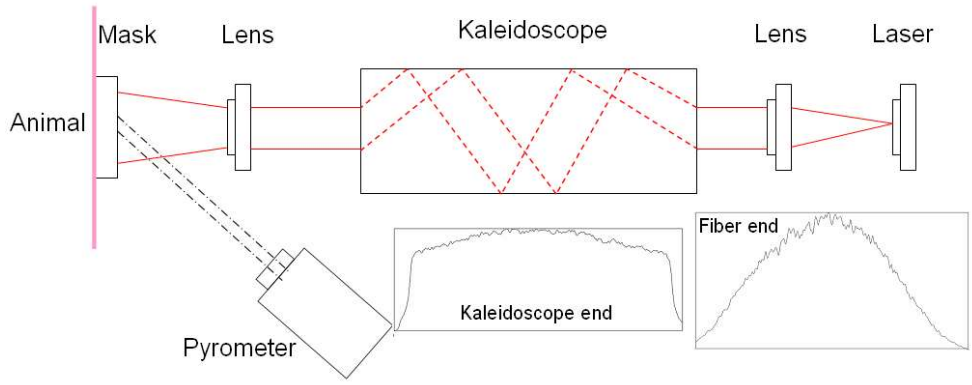

Fig. 3. Schema of the experimental setup and laser spatial distribution before and after the kaleidoscope.

The test bench setting up is complicated since the use of pyrometer which bandwidth (8-14 µm) contains the laser wavelength (10.6 µm). In these conditions, the pyrometer is saturated by reflections at this wavelength and measured values are not correct. So, a ZnSe window has been located before the pyrometer. The cavity between these two systems is filled with a gas absorbing this wavelength: SF_6. The laser spot images have been analyzed (EasyGrab, Scion Image and Origin 6.1 software) in order to verify the spatial uniformity of incident laser (an example is shown Fig. 3). In order to investigate potential damage induced by lasers, different irradiances and exposure durations (t_e) have been considered (Table 3). These experimental specificities have been chosen according to preparatory tests.

Table 3 Type of laser aggression (irradiance and duration).

	Duration (s)	Irradiance (10^4 W.m^{-2})				
Laser 1940 nm	$1 \le t_e \le 35$	0.9	1.1	1.2	1.4	
Laser 808 nm	$2 \le t_e \le 20$	0.9	1.4	9.6	11.0	12.2
Laser 10.6 µm	$0.25 \le t_e \le 20$	0.9	1.4	4.5	6.4	8.6

3.2 Protocol

The experimental protocol was approved by the consultative committee for ethics in animal experimentation of the French Army Biomedical Research Institute under the number 2008/14.0. Eight non pigmented female butcher pigs, weighing between 17.1 and 26.0 kg, were used in this study. A series of experiments were conducted *in vivo* on pig skin to induce thermal damage lesions using 808, 1940 and 10 600 nm lasers. Experimentations lasted three days as follows: laser exposures on day 1, clinical observation on day 2, and animal euthanasia and biopsies on day 3. In order to investigate the experimental reproducibility, experimentations were reproduced three times. Thus, twenty five burns of 2.25 cm^2 have been performed on flanks of each animal. Animals' medication and the biopsies' procedure are described in [2].

On day 1, after sedation by azaperone treatment (50 $mg.kg^{-1}$, Stresnil™, Janssen-Cilag) the animals were anesthetized by intramuscular injection of a combination of tiletamine and zolazepam (6 $mg.kg^{-1}$, Zoletil 100™, Virbac), and then kept under volatile anesthesia with a gas mixture of approximately 2% isoflurane (Isuflurane Belamont™, Mundipharma) in oxygen (1 $dm^3.min^{-1}$). To avoid animal pain, analgesia was given prior to laser exposure (10 $mg.1ml^{-1}$ of morphine) and extended all along the 3 days experiment with a transcutaneous patch of fentanyl (50 $\mu g.h^{-1}$, Durogesic™ 5 mg 10 cm^{-2} Janssen-Cilag). On day 3, animal euthanasia was performed by intravenous injection of 20 cm^3 of sodium pentobarbital (Dolethal™, Vétoquinol), and burns biopsies were harvested. The biopsies were fixed in neutral buffered 10% formalin solution (NBF) and stored at +2 8C/+8 8C. After fixation, the samples were dehydrated in alcohol solutions of increasing concentration, cleared in xylene and embedded in paraffin. Embedded biopsies were cut using a microtome (MICRON®, France). One section (5 µm thickness) per specimen was performed and stained with Hematoxylin Eosin Safran (HES). Qualitative and semi-quantitative histological evaluations of each biopsy were performed and the different parameters were graduated from 0 (absence) to 4 (severe). Moreover, burn severity is defined (Table 4) according to the French Society for Burn Study and Treatment (SFETB) classification (www.sfetb.org).

Table 4 SFETB classification

Histological grade	Description
1	Superficial epidermis involvement
2	Whole thickness epidermal involvement Basal membrane disruption Papillary dermis involvement
2+	Full-thickness epidermal necrosis, except for hair follicles Partial to complete basal membrane necrosis Reticular dermis involvement
3	Full-thickness epidermal necrosis, including hair follicles Complete basal membrane necrosis Deep dermis/hypodermis involvement

3.3 Experimental Results

Several figures presented in this section exhibit small oscillatory artefacts caused by electromagnetic interference (EMI). In order to avoid distortion of useful information in the figures by removing the EMI, the data in the figures is unfiltered. The artefacts caused by the EMI have a maximal amplitude of 2°C. Average initial temperature measured on eight pigs' skin is 32.4°C (standard deviation is 1.9°C). Three experimental campaigns have been performed and environmental conditions were:

- first campaign (I) : average room temperature: 22.3 °C ±0.3 °C, relative humidity 32%,
- second campaign (II) : average room temperature: 22 °C ±0.4 °C, relative humidity 31%,
- third campaign (III) : average room temperature: 22 °C ±0.5 °C, relative humidity 51%.

3.3.1 808 nm Laser

Several results previously obtained with this laser has been presented in [2]. Nevertheless, in order to complete these results, experimental conditions are summarised in Table 5 and maximal surface temperature is given. As foreseen, in the same conditions, the 808 nm laser induces less serious but deeper damage than any surfacic laser.

Table 5 Experimental conditions, maximal temperature of skin surface and biopsies results for 808 nm laser (first experimental campaign I)

Irradiance (x10^4 W.m^{-2})	Exposure duration (s)	Maximal surface temperature (°C) (mean on three measures)	Histological grade
0.9	10	37.9	0
0.9	20	38.6	0
1.6	5	38.1	0
1.6	10	37.1	0
1.6	20	40.3	0
9.6	5	43.7	1
9.6	10	52.1	1
11.0	5	46.3	1
11.0	10	55.3	1
12.2	2	40.8	0
12.2	5	43.4	0
12.2	8	47.3	0
12.2	10	49.8	2
12.2	15	55.0	2+
12.2	20	66.7	3

3.3.2 1940 nm Laser

In Fig. 4, temperature evolution of pig skin after the laser exposure is presented for several durations and for irradiance of 1.2 10^4 W.m^{-2}. It is obvious that thermal effect strongly depends on the exposure duration. For example, respectively for an exposure of 15 s, 10 s and 5 s, surface temperature increased by 35.5°C, 27.4°C and 17.5°C. Respectively, lesions are diagnosed 3 (severe burn), 2+ (deep second degree) and 0 (absence of lesion). The results of the biopsies of

the damaged tissues are presented in Table 6 for several exposure durations and irradiances.

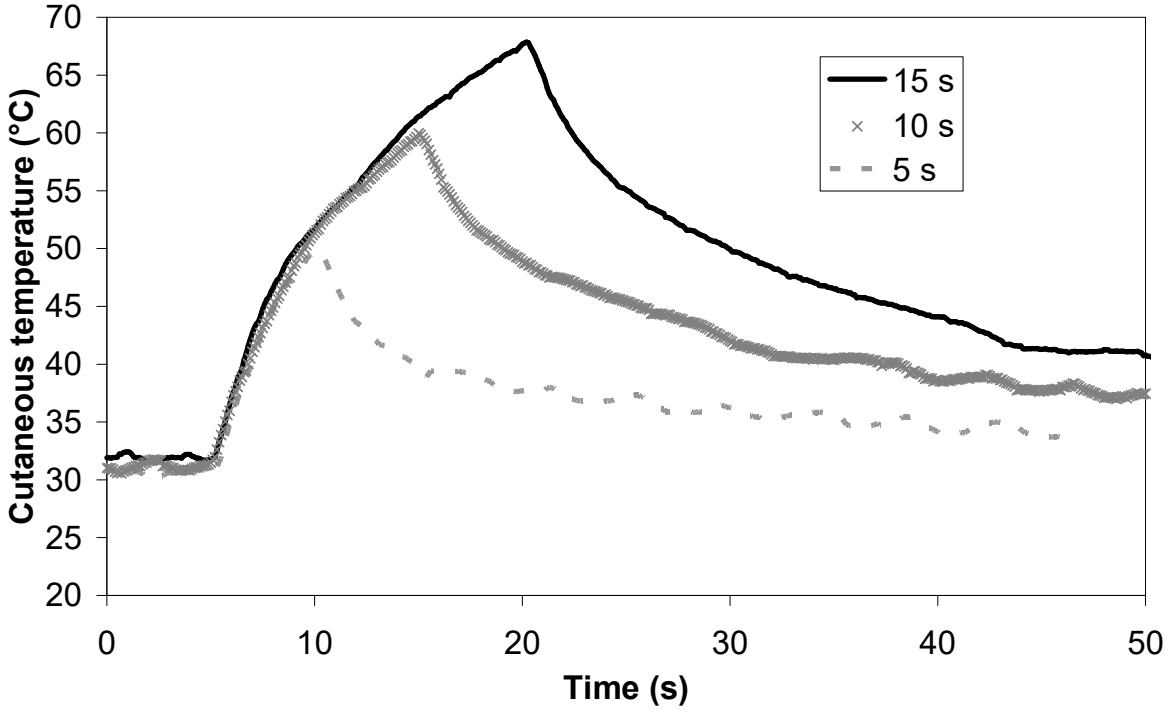

Fig. 4. Temperature evolution on skin surface: 1940 nm laser exposure, irradiance: 1.2 10^4 W.m^{-2}.

Table 6 Experimental conditions, maximal temperature of skin surface and biopsies results for 1940 nm laser (second and third experimental campaign II & III)

Irradiance (x10^4 W.m^{-2})	Exposure duration (s)	Maximal surface temperature (°C) (mean on three measures)	Histological grade	Experimental campaign
0.9	5	45.8	0	III
0.9	15	58.1	2+	III
0.9	20	70.5	2+	II
0.9	25	64.4	3	III
1.1	35	85.6	3	II
1.2	5	49.7	0	III
1.2	10	59.6	2+	III
1.2	15	67.5	2+	III
1.4	1	38.7	0	III
1.4	5	53.3	0	III
1.4	10	71.5	2+	II
1.4	15	75.0	3	II
1.4	20	82.7	3	II

3.3.3 10.6 µm Laser

In Fig. 5, temperature evolution of pig skin after laser exposure is presented for several durations (from 0.1 s up to 2s) and for 8.6 10^4 $W.m^{-2}$ irradiance. For the laser of 1940 nm, the increase of temperature and thermal effect depend of exposure duration. For this example, respectively, maximal cutaneous temperatures are 46.3, 56.5, 67.2, 78.6, 82.7 and 106.6°C for 0.1, 0.25, 0.5, 0.75, 1 and 2 s exposure times. Observed maximal temperatures and biopsies results are summarised in Table 7.

Table 7 Experimental conditions, maximal temperature of skin surface and biopsies results for 10 600 nm laser (second and third experimental campaign II & III)

Irradiance ($x10^4$ $W.m^{-2}$)	Exposure duration (s)	Maximal surface temperature (°C) (mean on three measures)	Histological grade	Experimental campaign
0.9	10	49.2	0	III
0.9	15	56.4	1	III
0.9	20	57.0	2+	II
0.9	25	57.4	3	III
1.4	1	37.0	0	III
1.4	5	49.7	0	III
1.4	10	60.2	2+	II
1.4	15	64.6	3	III
1.4	20	74.2	3	III
4.5	1	55.2	1	II
4.5	2	65.6	2+	II
6.4	0.1	41.0	0	II
6.4	0.5	49.5	1	II
6.4	0.75	65.9	2	II
6.4	1	66.7	2+	II
6.4	2	83.3	2+	II
6.4	3	96.1	3	III
8.6	0.1	47.7	0	II
8.6	0.25	55.0	1	II
8.6	0.5	65.4	2	II
8.6	0.75	76.5	2+	II
8.6	1	81.3	2+	II
8.6	2	103.8	3	III

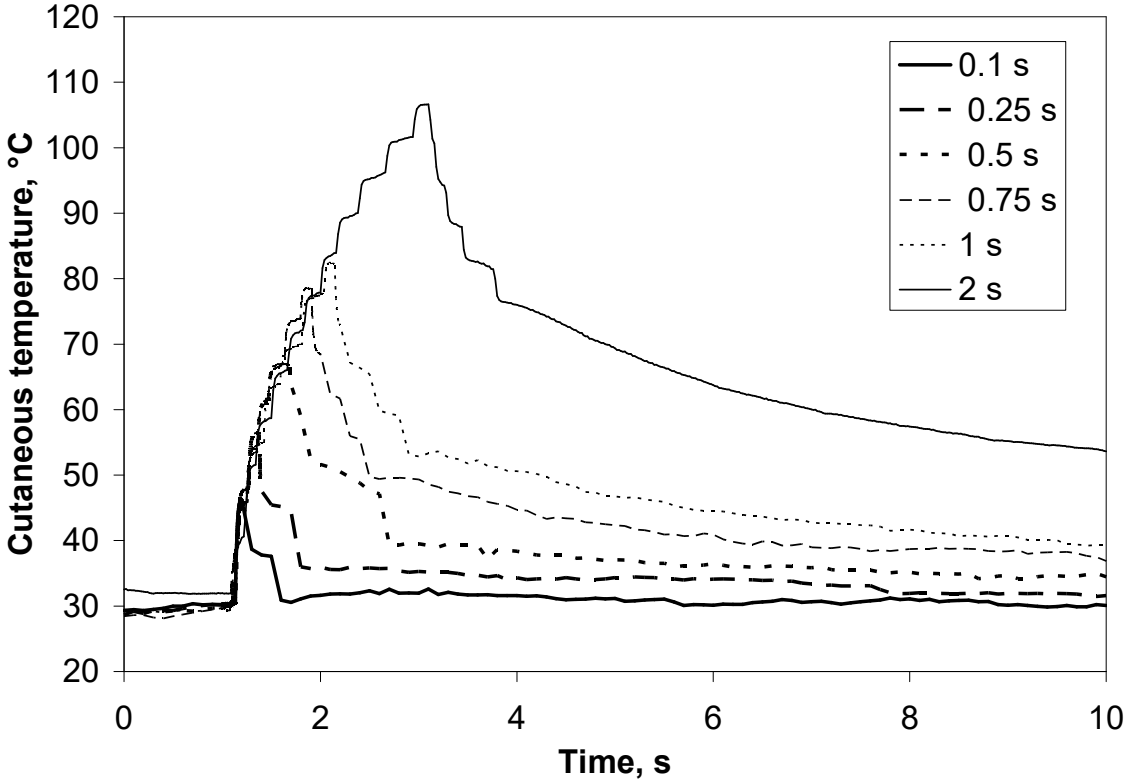

Fig. 5. Temperature evolution on skin surface: 10.6 µm laser exposure, irradiance: 8.6 10^4 $W.m^{-2}$.

3.3.4 Damage Comparison caused by Three Lasers (808, 1940 and 10600 nm)

In order to investigate injuries caused by lasers, different experiments (same irradiance and same exposure duration) have been compared and the evolutions of temperature are presented in Fig. 6. Laser of 808 nm has a slight influence on surface temperature compared with other wavelengths. In this example, maximal cutaneous temperatures are 37.0, 71.5 and 61.7°C respectively for lasers of 808, 1940 and 10 600 nm.

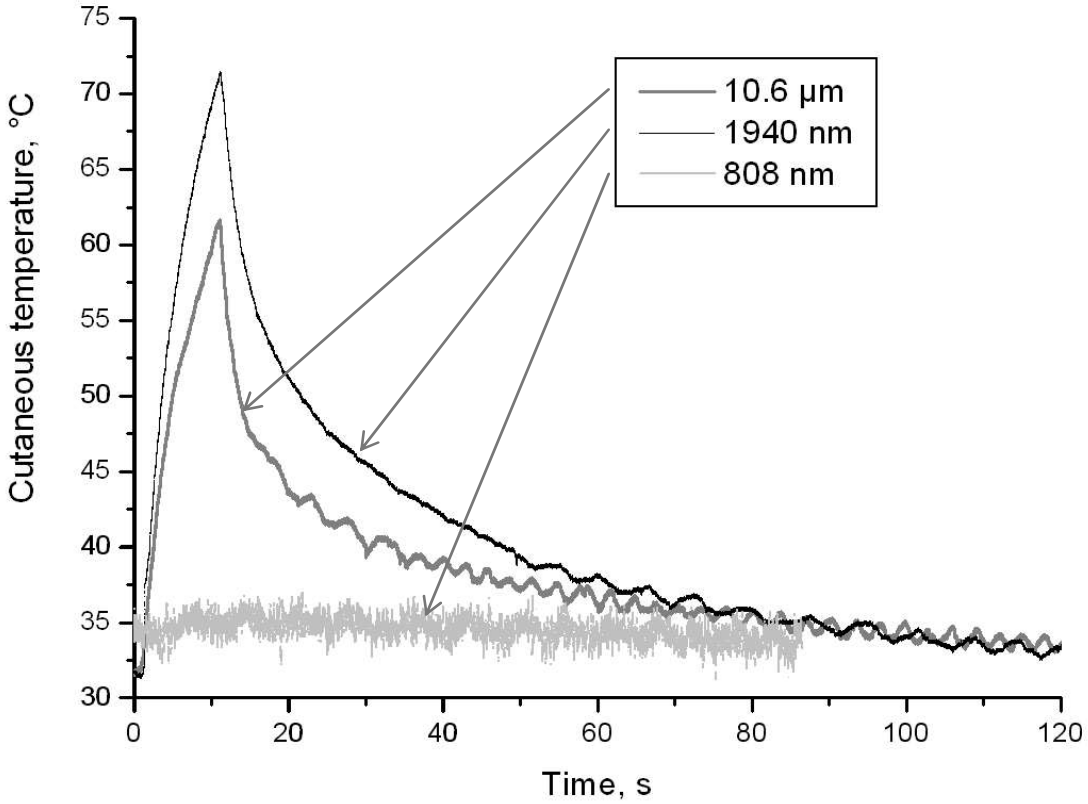

Fig. 6. Temperature evolution on skin surface for three laser (same duration and same irradiance).

4 Discussion

In the investigated situation, the damage corresponds respectively for the lasers of 808, 1940 nm and 10.6 µm to an absence of lesion, third degree and deep second degree burn. Experimental results are contradicted by literature results. According to literature [33], the 1940 nm laser should be more superficial than 808 nm; which was confirmed by our experimental results. But literature also states that the 10.6µm should be more superficial than the 1940 nm laser, which is contradicted in our fourth experimental campaign shown Fig. 6.
According to several physiological parameters involved in burn process (vasodilatation, vasoconstriction, water losses, substance losses, etc.), it is quite difficult to validate mathematical predictive model without considering *in vivo* configurations.

4.1 Comparison between Simulated and Experimental Temperatures

On Fig. 7, several results are presented in order to compare temperatures issued from

mathematical predictive model and measured temperatures (using infrared pyrometer). Three lasers are studied for two spot duration and two irradiances.

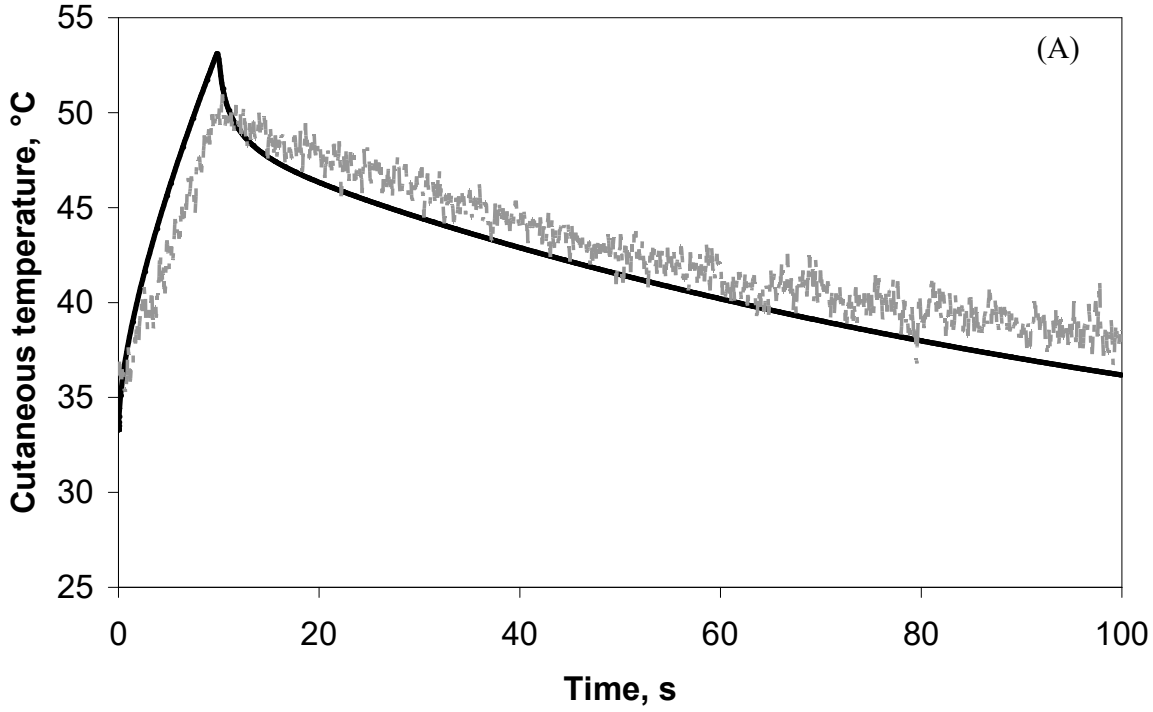

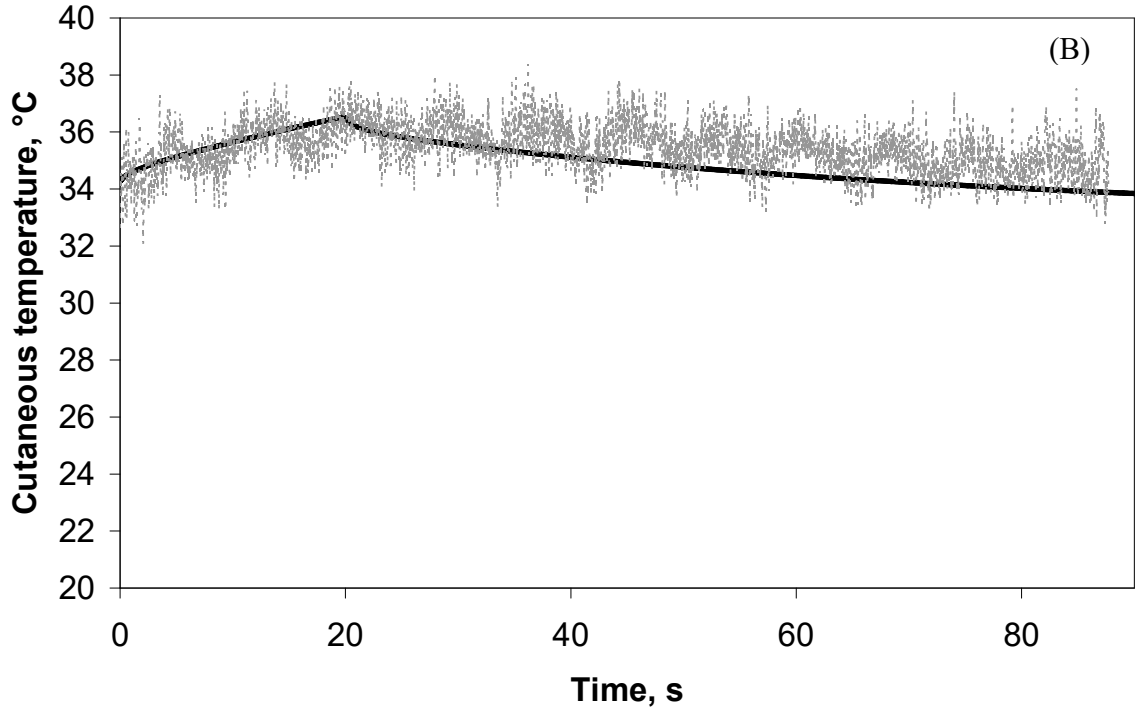
(B)
Cutaneous temperature, °C
40
38
36
34
32
30
28
26
24
22
20
0
20
40
60
80
Time, s

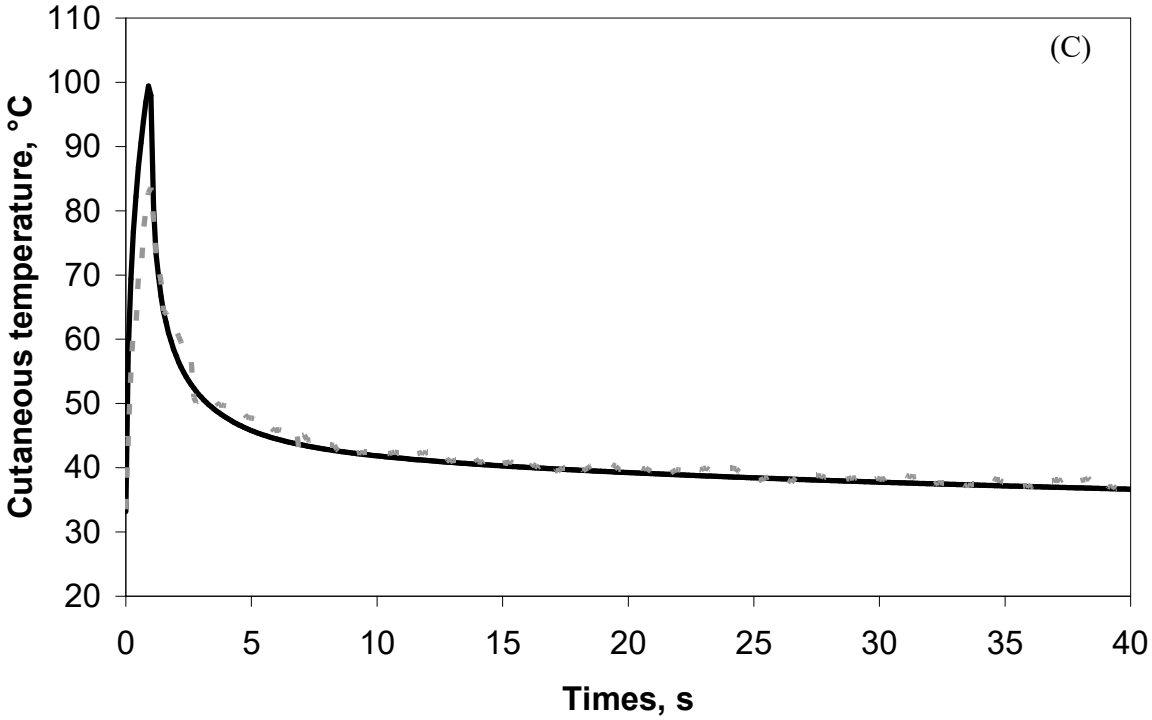
(C)
Cutaneous temperature, °C
110
100
90
80
70
60
50
40
30
20
0
5
10
15
20
25
30
35
40
Times, s

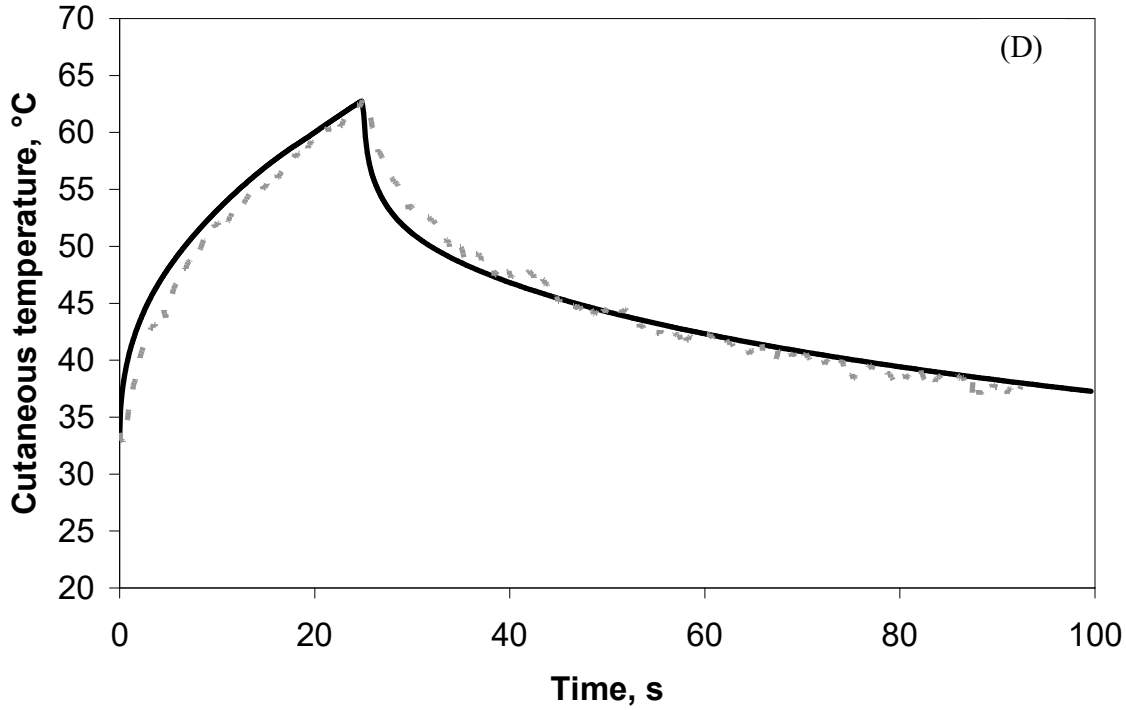
(D)
Cutaneous temperature, °C
Time, s
70
65
60
55
50
45
40
35
30
25
20
0
20
40
60
80
100

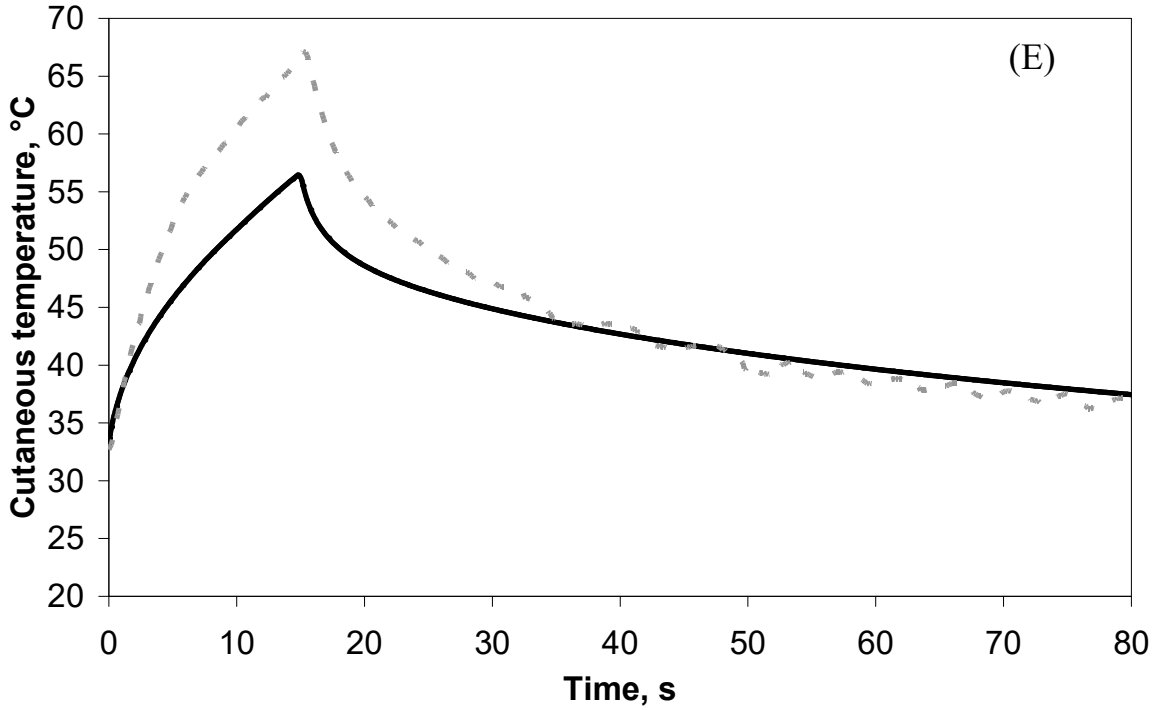
(E)
Cutaneous temperature, °C
Time, s
70
65
60
55
50
45
40
35
30
25
20
0
10
20
30
40
50
60
70
80

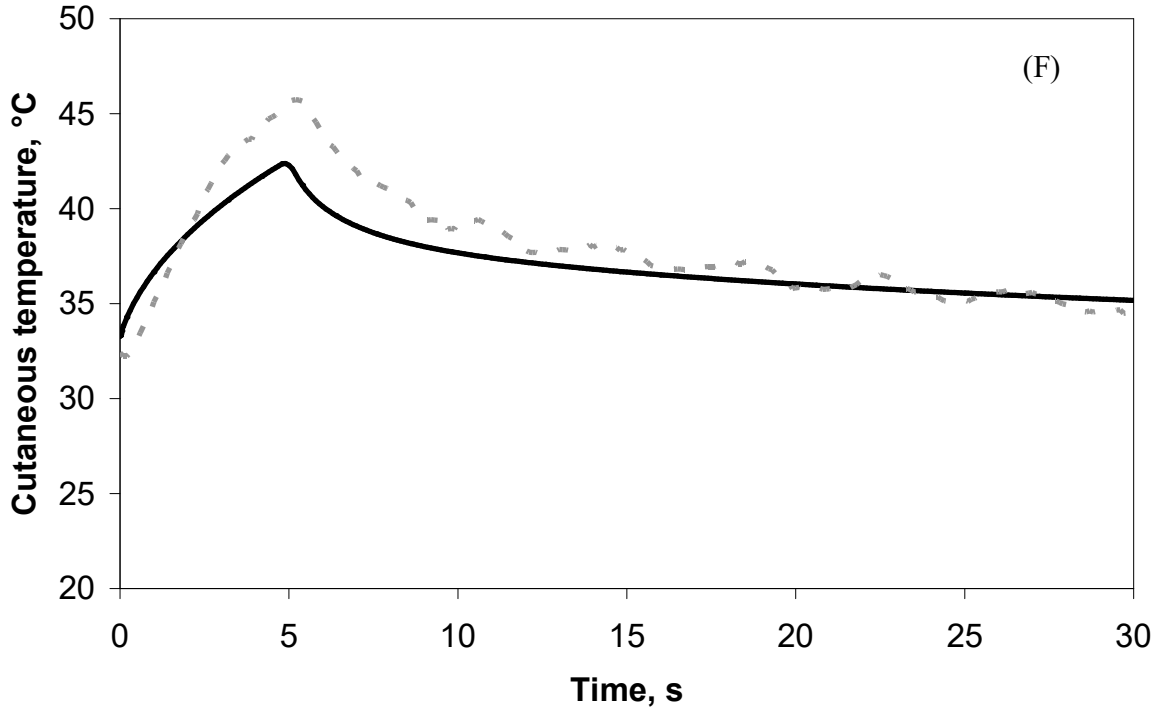

Fig. 7. Experimental (grey) and predicted (black) temperatures for several laser aggressions. (A) Laser 808 nm – 12.2 10^4 W.m^{-2} – 10s, (B) Laser 808 nm – 0.9 10^4 W.m^{-2} – 20s, (C) Laser 10.6 µm – 8.6 10^4 W.m^{-2} – 1s, (D) Laser 10.6 µm – 0.9 10^4 W.m^{-2} – 25s, (E) Laser 1940 nm – 1.2 10^4 W.m^{-2} – 15s, (F) Laser 1940 nm – 0.9 10^4 W.m^{-2} – 5s.

Considering Fig 7, the following remarks are proposed:

- 808 nm laser: during the heating stage, the simulation seems to slightly overestimate the temperature evolution.
- 10.6 µm laser: model seems to overestimate cutaneous temperatures particularly when exposure times are short (0.25 to 1 s). For longer exposures, simulated and experimental temperatures are similar.
- 1940 nm laser: calculated temperatures are underestimated during the heating process.

Model results for the 808 nm aggression are in good agreement with cutaneous temperature measurements. Concerning 1940 nm and 10.6 µm laser aggressions, some improvements are to be brought. The only difference between simulations performed for these two wavelengths is due to the extinction coefficient (β) and more precisely, water absorption coefficient (μ_{water}) which is higher for 10.6 µm than for 1940 nm. It explains why the first is more superficial than the second one. Nevertheless, during animal experimentations, cutaneous temperatures were higher for 1940 nm laser aggression. If the coefficient extinction is modified inside the model (increased for 1940 nm laser or decreased for 10.6 µm laser), the agreement between simulated and

experimental results on skin surface is not significantly affected. It is obvious that other non neglectable biological phenomenon must interfere (such as inflammation, edema, electrolytic unbalance, etc.).

4.2 Comparison between Simulated and Experimental Damages

According to the parameters proposed by several authors [13, 30, 37-41], it is quite difficult to define an optical set of values for A and E_a. In fact, concerning the laser of 1940 nm, Henriques and Takata's parameters allow correct prediction [30,13], for 10.6 µm, Weaver and Stoll and Gaylor (according to simulation conditions) return the best prediction [38,39], and finally, for 808 nm laser, only Gaylor's values give correct results [39]. On the other hand, cutaneous experimental temperatures are not necessarily the highest among the layers. So, it is difficult to draw conclusions on the damage prediction from these temperatures. According to the modeling and depending on wavelength, during a thermal aggression the highest temperatures are located in the epidermis or in the dermis. Such behavior is illustrated Fig. 8 for two configurations.

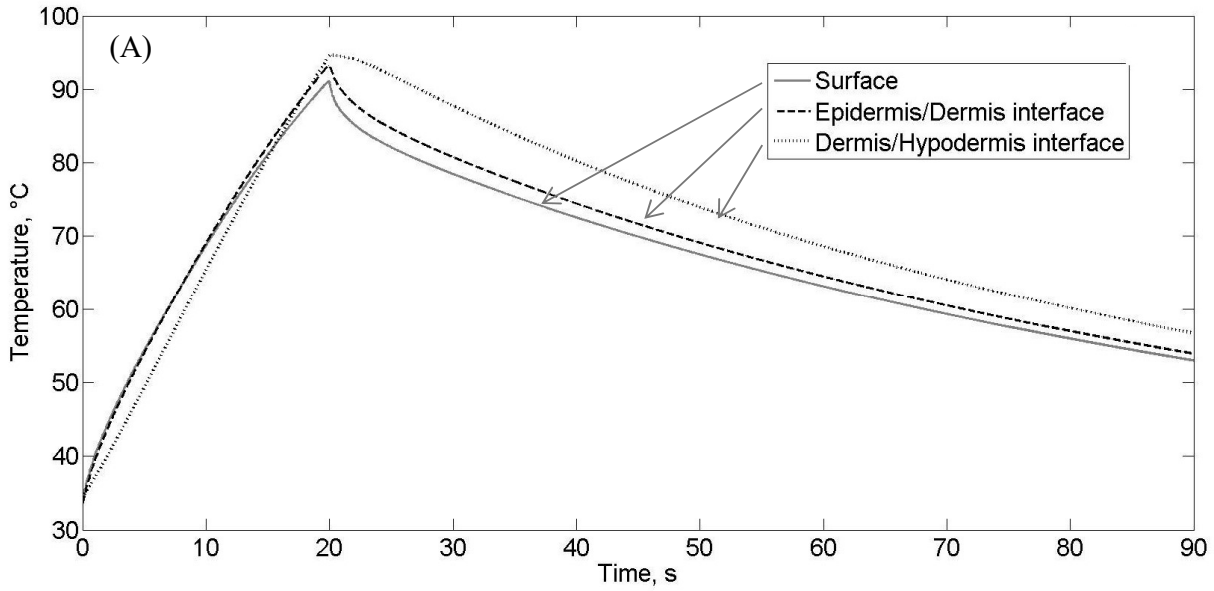

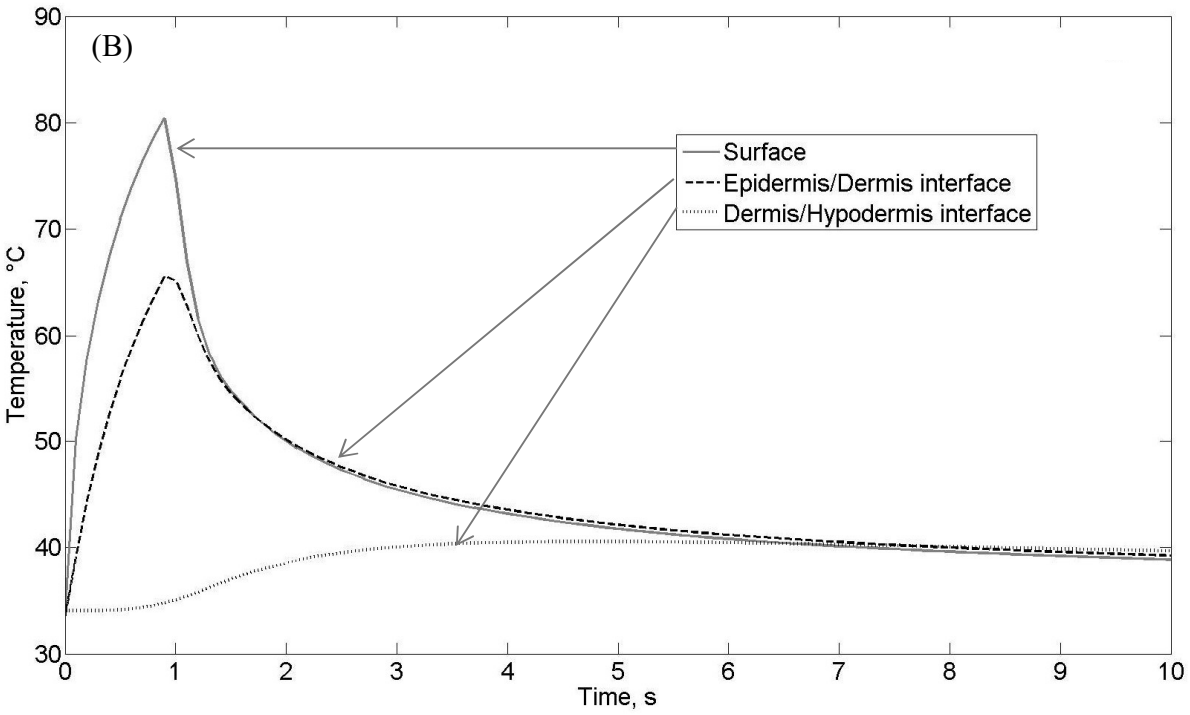

Fig. 8. Simulated temperatures evolution at skin interfaces. (A) Laser 808 nm – 12.2 10^4 W.m^{-2} – 20s, (B) Laser 10.6 µm – 6 10^4 W.m^{-2} – 1s.

The prediction based on surface temperatures could be underestimated. Precisely, concerning the 1940 nm laser, this study is based on Chen et al.'s research [5,33]. These authors show that Gaylor's parameters predict a damage similar to their histological observations. However, they noticed a variation which cause is attributed to optical and thermal parameters diversity of different animals. Nevertheless, the comparison between the histological damage (biopsies) and the evolution of simulated temperatures can enable to predict generated damages. Tables 8 to 10 present these predictions according to time of exposure and irradiations. As previously explained, the laser of 808 nm is less dangerous than the two other tested wavelengths. Indeed, for irradiation of 8.10^4 W.m^{-2}, the necessary exposure time to get a 3rd degree burn is 30 s for the 808 nm laser and 1 s for the 10.6 µm laser.

Table 8 Damage predictions according to exposition time and to irradiation for the 1940 nm laser

Irradiation	**Exposition time (s)**							
(x 10^4 W.m^{-2})	**1**	**2**	**5**	**10**	**15**	**20**	**25**	**30**
0.5	0	0	0	0	0	0	0	0
0.9	0	0	0	0	2	2	2	2
1	0	0	0	1	2	2	2	3
1.1	0	0	0	1	2	2	3	3
1.2	0	0	0	2	2	3	3	3
1.3	0	0	0	2	2	3	3	3
1.4	0	0	0	2	3	3	3	3

Table 9 Damage predictions according to exposition time and to irradiation for the 10.6 µm laser

Irradiation	**Exposition time (s)**											
(x 10^4 W.m^{-2})	**0.1**	**0.25**	**0.5**	**0.75**	**1**	**2**	**5**	**10**	**15**	**20**	**25**	**30**
0.5	0	0	0	0	0	0	0	0	0	1	2	2
0.9	0	0	0	0	0	0	0	0	2	2	2	2
1	0	0	0	0	0	0	0	1	2	2	2	2
1.2	0	0	0	0	0	0	0	2	2	2	2	3
1.4	0	0	0	0	0	0	0	2	3	3	3	3
1.6	0	0	0	0	0	0	1	2	3	3	3	3
1.8	0	0	0	0	0	0	2	2	3	3	3	3
2	0	0	0	0	0	0	2	2	3	3	3	3
2.5	0	0	0	0	0	1	2	2	3	3	3	3
3	0	0	0	0	0	2	2	3	3	3	3	3
3.5	0	0	0	0	1	2	2	3	3	3	3	3
4	0	0	0	0	1	2	2	3	3	3	3	3
4.5	0	0	0	1	1	2	3	3	3	3	3	3
5	0	0	0	2	2	2	3	3	3	3	3	3
5.5	0	0	1	2	2	2	3	3	3	3	3	3
6	0	0	2	2	2	3	3	3	3	3	3	3
6.5	0	0	2	2	2	3	3	3	3	3	3	3
7	0	0	2	2	2	3	3	3	3	3	3	3
7.5	0	0	2	2	2	3	3	3	3	3	3	3
8	0	1	2	2	3	3	3	3	3	3	3	3
8.6	0	1	2	2	3	3	3	3	3	3	3	3

Table 10 Damage predictions according to exposition time and to irradiation for the 808 nm laser

Irradiation	**Exposition time (s)**					
(x 10^4 W.m^{-2})	**5**	**10**	**15**	**20**	**25**	**30**
1	0	0	0	0	0	0
1.4	0	0	0	0	0	0
1.6	0	0	0	0	0	1
2	0	0	0	0	1	2
2.5	0	0	0	1	2	2
3	0	0	1	2	2	2
3.5	0	0	2	2	2	2
4	0	0	2	2	2	2
4.5	0	1	2	2	2	2
5	0	2	2	2	2	2
5.5	0	2	2	2	2	2
6	0	2	2	2	2	2
6.5	0	2	2	2	2	2
7	0	2	2	2	2	2
7.5	0	2	2	2	2	2
8	0	2	2	2	2	3
8.5	1	2	2	2	2	3
9	1	2	2	2	3	3
9.5	1	2	2	2	3	3
10	1	2	2	2	3	3
10.5	1	2	2	2	3	3
11	1	2	2	3	3	3
11.5	1	2	2	3	3	3
12.2	1	2	2	3	3	3

4.3 Damage modeling for different body parts

In the mathematical predictive model, skin layers thicknesses are easy to modify. According to the literature, the thicknesses of face skin are respectively 0.05 mm, 0.6 mm and 0.8 mm for the epidermis, dermis and hypodermis [42]. For the hand palm, thicknesses are 1 mm, 2 mm and 1 mm [25]. Results for both these body parts with the laser of 10.6 µm are presented (Fig. 9). According to the simulation, it seems that the damage of the face is sensibly the same than the damage of the arm, whereas the lesion of the hand will be more important. It seems that, the thicker the epidermis is, the more the surface temperature rises. The epidermis being an insulator, the dissipation of heat in depth is more difficult.

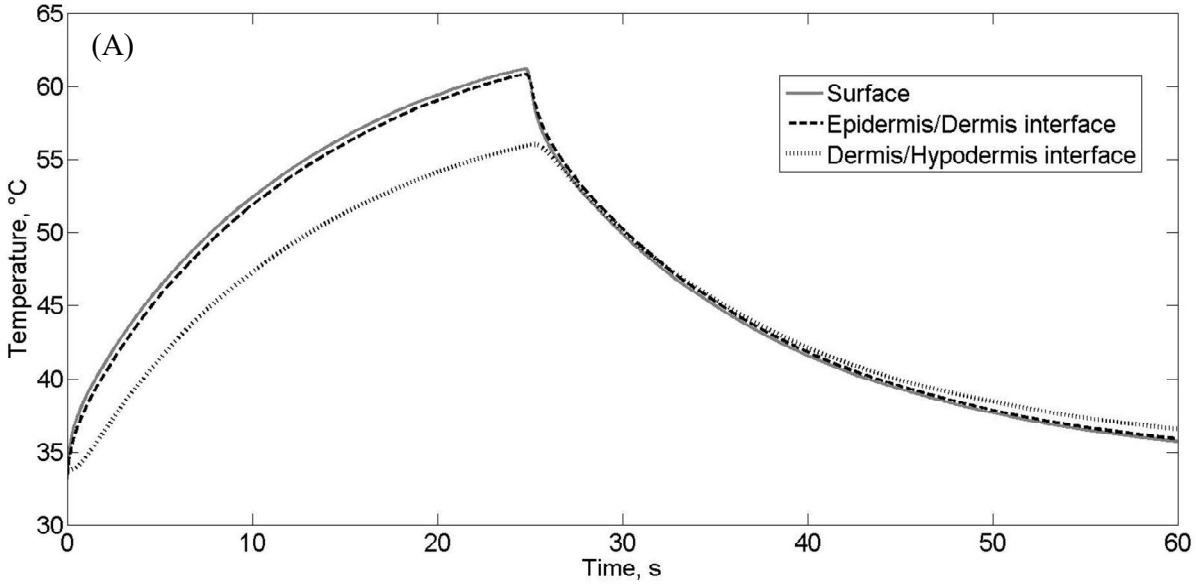
(A)
Surface
Epidermis/Dermis interface
Dermis/Hypodermis interface
Temperature, °C
Time, s
65
60
55
50
45
40
35
30
0
10
20
30
40
50
60

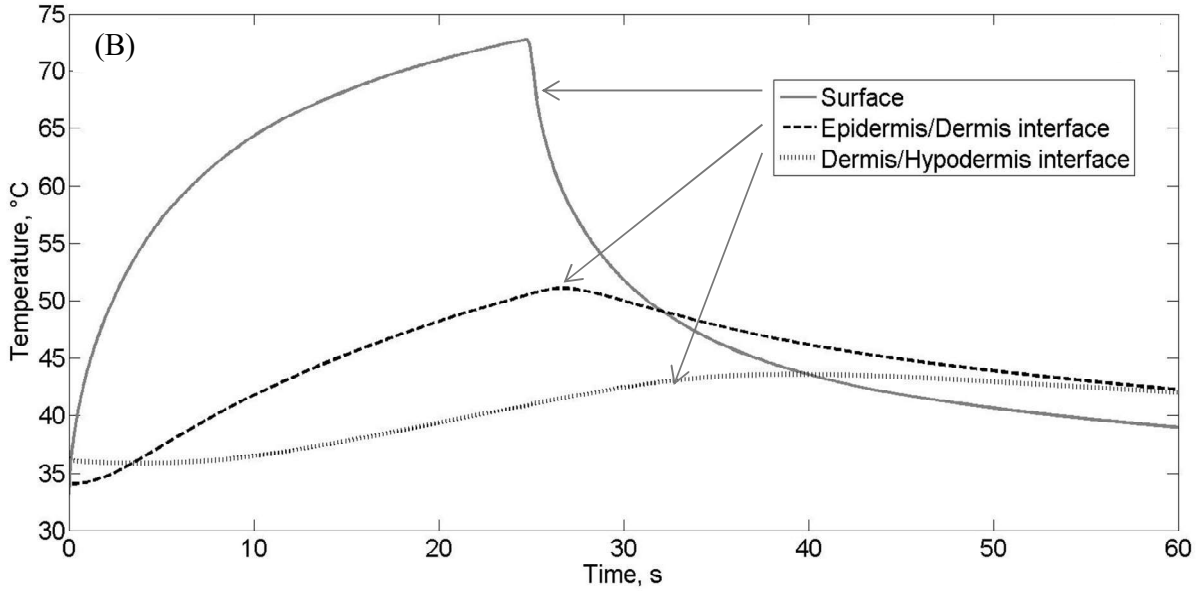
(B)
Surface
Epidermis/Dermis interface
Dermis/Hypodermis interface
Temperature, °C
Time, s
75
70
65
60
55
50
45
40
35
30
0
10
20
30
40
50
60

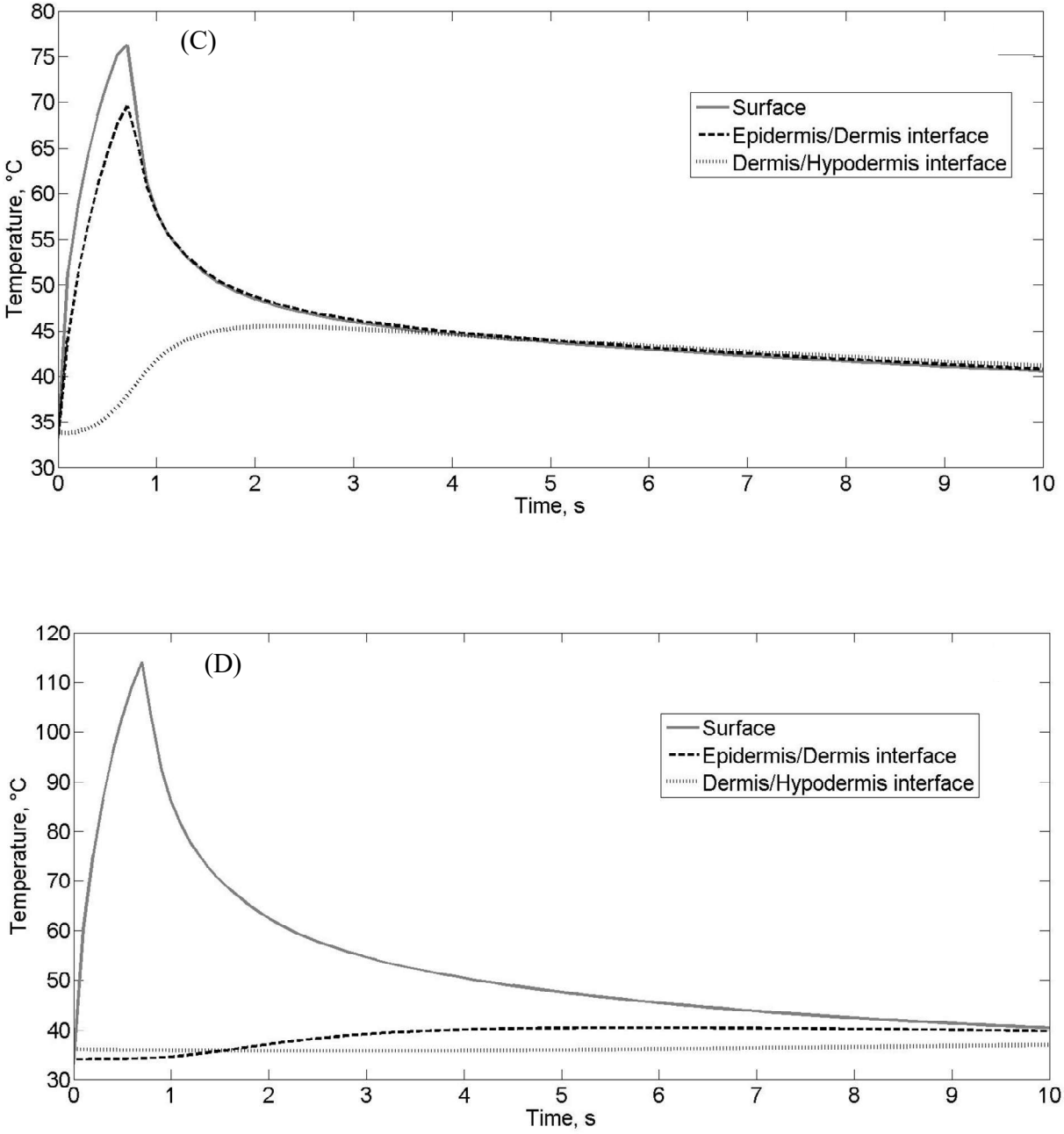

Fig. 9. Simulated temperatures evolution of skin interfaces for face and palm of hand (laser 10.6 µm). (A) Face – 0.9 10^4 W.m^{-2} – 25 s, (B) Hand palm – 0.9 10^4 W.m^{-2} – 25 s, (C) Face – 8.6 10^4 W.m^{-2} – 0.75 s, (D) Hand palm – 8.6 10^4 W.m^{-2} – 0.75 s.

5. Concluding remarks

Considering three lasers (808 nm, 1940 nm and 10.6 µm), *in vivo* experimentations have been performed on pigs in order to investigate several aggression durations and powers. Simultaneously, a mathematical model has been developed and different physiological phenomena as blood flow evolution and water losses are taken into account in order to improve the prediction of measured temperatures during the cooling phase. Concerning the heating phase, numerical simulations are relevant for laser of 808 nm, but for the two other lasers, some improvements have to be brought. Extinction coefficient does not seem to be the only responsible of the weak adequacy between experimental and simulated results. One of the assumptions could be that as the laser goes relatively deeply in the dermis (with higher hydration rate), under the effect of the laser aggression a tissue separation occurs, or even an edema is induced and add an insulative layer. Aggression pursuit and/or heat accumulation lead to skin surface temperature increase. Besides physiological parameters which are difficult to control, burn phenomena modeling is usually based on rough assumption: skin is globally defined as a stacking of three homogeneous layers, however, tissues are constituted of thousands of cells and various molecules. Interfaces are not regular on all layer's length, but present irregularities caused, for example, by dermis papillary area. Finally, in this study, the model validity can only be verified by non-intrusive measurements on skin surface.

Nevertheless, comparing histological and simulated results, it is possible to predict burn depending on time and irradiation. In such a aim, simulations have been required to detect the best values for A and E_a parameters. According the wavelength, results are different. Actually damage parameters have been defined with specific experimental protocols (tissues, animals, molecules, in vitro experimentations …). Results presented here can not be extrapolated for other wavelengths and other irradiation powers but similar lesions can be generated by different infrared lasers. Mathematical model also enables to predict temperature evolution in three layers of skin and it seems possible to simulate skin temperature for different regions of body. The main difference is layer thickness. So, these simulations show that the thicker the epidermis is, the more the surface temperature increases. In a near future, it would be interesting to verify this observation *in vivo* and to test other wavelength although, to a certain extent, this mathematical model permits to avoid animal experimentation.

References

1. E.F. Maher, in *Report SAM-TR-78-32*: *Transmission and absorption coefficients for ocular media of the Rhesus monkey*. San Antonio, TX: Brooks Air Force Base (1978)
2. N. Museux, L. Perez, L. Autrique, D. Agay, Burns 38, 658 (2012)
3. S.D. Jackson, A. Lauto, Lasers Surg. Med. **30**, 184 (2002)
4. S.L. Jacques, Appl. Opt. **32**, 2447 (1993)
5. B. Chen, D.C. O'Dell, S.L. Thomsen, B.A. Rockwell, A.J. Welch, Lasers Surg. Med. **37**, 373 (2005)
6. B. Choi, J.K. Barton, E.K. Chan, A.J. Welch, Lasers Surg. Med. **23**,185 (1998)

7. B.M. Hantash, V.P. Bedi, B. Kapadia, Z. Rahman, K. Jiang, H. Tanner , K.F. Chan, Lasers Surg. Med. **39**, 96 (2007)
8. B.P. Payne, N.S. Nishioka, B.B. Mikic, V. Venugopalan, Lasers Surg. Med. **23**, 1 (1998)
9. A.J. Welch, J.H. Torres, W.F. Cheong, Texas Heart Institute Journal. Physics, System design, Experimental applications, **16**, 141 (1989)
10. T.P. Sullivan, W.H. Eaglstein, S.C. Davis, P. Mertz, Wound Rep. Reg. **9**, 66 (2001)
11. H.H. Pennes, J. Appl. Physiol. **85**, 5 (1948)
12. B. Chen, S.L. Thomsen, R.J. Thomas, J. Oliver, A.J. Welch, Lasers Surg. Med. **40**, 358 (2008)
13. A.R. Moritz, F.C. Henriques, Am. J. Pathol. **23**, 695 (1947)
14. F.F. Henriques, Arch. Pathol. **43**, 489 (1947)
15. A. Shitzer, M.K. Kleiner, *Thermal behavior of biological tissues – a general analysis*, Bulletin of mathematical biology, **38**, (1976)
16. M.M. Chen, K.R. Holmes, *Microvascular contributions in tissue heat transfer*, Annals New York Academy of sciences, **335**, 137-150, (1980)
17. S. Weinbaum, L.M. Jiji, D.E. Lemons, *Theory and experiment for the effect of vascular microstructure on surface tissue heat transfer. Part I: anatomical foundation and model conceptualization*, ASME J. Biomech. Eng. **106**, 321–330, (1984)
18. J. Lang, B. Erdmann, M. Seebass, *Impact of Nonlinear Heat Transfer on Temperature Control in Regional Hyperthermia*. IEEE Transactions on Biomedical Engineering, **46**, 1129-1138, (1999)
19. D.T. Tompkins, R. Vanderby, S.A. Klein, W.A. Beckman, R.A. Steeves, D.M. Frye, B.R. Paliwal, *Temperature-Dependent versus Constant-Rate Blood Perfusion Modelling in Ferromagnetic Thermoseed Hyperthermia: Results with a Model of the Human Prostate*, International Journal of Hyperthermia, **10**, 517-536, (1994)
20. B. Erdmann, J. Lang, M. Seebass, *Optimization of Temperature Distributions for Regional Hyperthermia Based on a Nonlinear Heat Transfer Model*, Annals of the New York Academy of Sciences, **858**, 36-46, (1998)
21. E. Kengne, I. Mellal, M. Ben Hamouda, A. Lakhssassi, *A Mathematical Model to Solve Bio-Heat Transfer Problems through a Bio-Heat Transfer Equation with Quadratic Temperature-Dependent Blood Perfusion under a Constant Spatial Heating on Skin Surface*, Journal of Biomedical Science and Engineering, **7-9**, (2014)
22. D. Fiala, K.J. Lomas, M. Stohrer, *A computer model of human thermoregulation for a wide range of environmental conditions: the passive system*, J. Appl. Physiol. **87**, 1957-1972, (1999)
23. J.P. Abraham, E.M. Sparrow, Int. J. Heat Mass. Trans. **50**, 2537 (2007)
24. M. Knudsen, J. Overgaard, IEEE Trans. Biomed. Eng. **33**, 477 (1986)
25. C. Lormel, Ph.D. thesis (Perpignan, France 2005)
26. H.S. Carslaw ,J.C. Jaeger, Conduction of Heat in solids, Oxford science publications, second edition, 1946.
27. F.P. Incropera, D.P. Dewitt, in *Fundamentals of Heat and mass transfer*, 5th edn. (John Wiley & Sons, New York, 2001)
28. J.H. Torres, M. Motamedi, J.A. Pearce, A.J. Welch, Appl. Opt. **32**, 597 (1993)

29. S.H. Diaz, G. Aguilar, E.J. Lavernia, B.J.F. Wong, IEEE J. Quantum Electron **7**, 944 (2001)
30. A. Takata, Aerospace Med. **45**, 634 (1974)
31. J.Z. Zhang, Y.G. Shen, X.X. Zhang, Lasers Med Science **24,** 329 (2009)
32. H.S. Hatfield, J. Physiol. **120**, 35 (1953)
33. B. Chen, S.L. Thomsen, R.J. Thomas, A.J. Welch, J. Biomed. Opt. **11,** 6 (2006)
34. L. Autrique, C. Lormel, *Numerical design of experiment for sensitivity analysis - application to skin burn injury prediction*, IEEE Trans Biomed Eng., **55**(4):1279-90, (2008)
35. F. Breaban, J.F. Coutouly, P. Deprez, A. Deffontaine, Lasers Eng. **11**,77 (2001)
36. S. Mordon, in *Groupe laser de la Société Française de Dermatologie : les lasers en dermatologie*, 2st edn. (Doin, France, 2006)
37. Y.C. Wu, National Bureau of Standards, Washington, District of Columbia (1982)
38. J.A. Weaver, A.M. Stoll, in *NADC Memo Report 6708* (United Stated Naval Air Development Center, Johnsville, Pennsylvania, 1967)
39. D.C. Gaylor, Ph.D. thesis (Massachusetts Institute of Technology, USA, 1989)
40. J.A. Pearce, S.L. Thomsen, H. Vijverberg, T.J. McMurray, in Proc SPIE: *Kinetics for birefringence changes in thermally coagulated rat skin collagen*, vol 1876, (1993), pp.180-185
41. C.E. Fugitt, in *Armed Forces Special Weapons Project AFSWP-606: A rate process of thermal injury* (1955)
42. J. Whitton, J. Everall, British J. Derm. **89**, 467 (1973)